Biol. Cybern. 80, 309–326 (1999)

Biological Cybernetics

A joint interspike interval difference stochastic spike train analysis: detecting local trends in the temporal firing patterns of single neurons

Michelle A. Fitzurka[1], **David C. Tam**[2]

[1] Department of Medical Physics, University of Wisconsin, Madison, WI 53705, USA
[2] Center for Network Neuroscience and Department of Biological Sciences, University of North Texas, Denton, TX 76203, USA

Received: 13 May 1997 / Accepted in revised form: 9 December 1998

Abstract. We introduce a stochastic spike train analysis method called joint interspike interval difference (JISID) analysis. By design, this method detects *changes* in firing interspike intervals (ISIs), called local trends, within a 4-spike pattern in a spike train. This analysis classifies 4-spike patterns that have similar incremental changes. It characterizes the higher-order serial dependence in spike firing relative to changes in the firing history. Mathematically, this spike train analysis describes the statistical joint distribution of consecutive changes in ISIs, from which the serial dependence of the changes in higher-order intervals can be determined. It is similar to the joint interspike interval (JISI) analysis, except that the joint distribution of consecutive ISI differences (ISIDs) is quantified. The graphical location of points in the JISID scatter plot reveals the local trends in firing (i.e., monotonically increasing, monotonically decreasing, or transitional firing). The trajectory of these points in the serial-JISID plot traces the time evolution of these trends represented by a 5-spike pattern, while points in the JISID scatter plot represent trends of a 4-spike pattern. We provide complete theoretical interpretations of the JISID analysis. We also demonstrate that this method indeed identifies firing trends in both simulated spike trains and spike trains recorded from cultured neurons.

1 Introduction

We introduce a stochastic spike train analysis technique to detect and characterize the sequential changes in a series of spike firings generated by individual neurons. Spike firings are traditionally represented by a time-series of action potentials called spike trains. A spike train can be treated as a point process (Perkel et al. 1967a, b) based on the classical theories of stochastic point processes (Correia and Landolt 1977; Cox and Lewis 1966; Gerstein and Kiang 1960; Gray 1967; Moore et al. 1966, 1970; Tuckwell 1988; Yang and Chen 1978). The firing characteristics of a neuron can be described by the temporal pattern of spike occurrences, which is quantified by the time sequence of spike occurrences (see Sect. 3.1). Although a temporal pattern can include any number of spikes, in this paper we examine patterns that are limited to a sequence of less than six consecutive spikes. Specifically, we characterize the changes within the temporal patterns, which we call 'local trends.' Other long-term trends can be analyzed using many of the traditional time-series analyses (e.g., Brillinger 1975; Gotton 1981; Sugihara 1994).

We are interested in analyzing the local trends within a short sequence of spikes for the following reasons. Specific temporal patterns of a neuron may encode significant information (Segundo et al. 1963; Sherry and Klemm 1982, 1984; Terasawa et al. 1989; Tsukada et al. 1975, 1982, 1983). Different sequences of spike firings may represent different encoding schemes, which may reflect changes in the dynamics of a neuron and/or changes in the signal content encoded by the firing patterns. Therefore, analysis of the local trends can potentially provide insight into the encoding properties of neurons in the central nervous system.

Limiting the analysis to short patterns may reveal the serial relationship between consecutive spike firings from which the statistical dependence of a stochastic process can be established. If a neuron obeys a simple Markov process in which the occurrence of the next event is dependent only on the present state and is independent of all of its past states, then the serial dependence relationship of two consecutive intervals is sufficient to describe the neuron's firing. The analysis of a 3-spike pattern (which includes two interspike intervals, ISIs) is adequate. If, however, the neuron follows a higher-order dependence process, then the serial dependence between more than two consecutive intervals is required. In this

Correspondence to: D.C. Tam, Department of Biological Sciences, University of North Texas, P. O. Box 305220, Denton, TX 76203–5220, USA
(e-mail: dtam@unt.edu,
Tel.: +1-940-565-3261, Fax: +1-940-565-4136)

case, an analysis will be needed that examines patterns that include more than three spikes (i.e., a 4-or-more spike pattern). Although a matrix equation for computing the higher-order transition probabilities from lower-order ones can be obtained from the Chapman-Kolmogorov equation for a Markov chain, we are particularly interested in the extent of the dependence of an unknown process on its specific history. The extent of this dependence can be quantified by the higher-order transition probabilities (or the conditional probabilities on its past series of histories), especially when the higher-order serial dependence is nonlinear. In contrast to the transition probabilities quantified by most traditional serial dependence analyses, we characterize the higher-order dependence by the changes in conditional probabilities.

Classically, a point process, such as a spike train, can be analyzed using random variables such as the nth spike occurrence at time, t_n, or the nth interspike interval, τ_n. An ISI is defined as the time difference between consecutive spikes, $\tau_n = t_n - t_{n-1}$. A higher-order ISI is defined as the time interval that spans multiple ISIs. Univariate statistics can be obtained based on this first-order ISI and/or other higher-order ISIs, such as autocorrelation in which all orders of ISIs are included in the analysis (Perkel et al. 1967a).

Bivariate statistics are often used to establish the relationship between two random variables (such as τ_n and τ_m) to determine serial dependence. Classical stochastic spike train analyses exploring the relationship between consecutive first-order ISIs (τ_n and τ_{n+1}) are called joint-ISI (JISI) plots (Rodieck et al. 1962; Schulman and Thorson 1964; Segundo et al. 1966). The statistical distribution of this first-order ISI pair (τ_n, τ_{n+1}) represents a two-dimensional ISI statistical distribution, or a joint-ISI distribution. This JISI analysis establishes the serial correlation of adjacent points in the time-series from which the joint probability of serial firings can be obtained by statistically estimating the transition probabilities. Recently, the same analysis has been re-examined in terms of deterministic chaos theories of nonlinear dynamics in which the JISI plots are referred to as 'interval return maps' (Nomura et al. 1994; Segundo et al. 1994; e.g., Selz and Mandell 1992; Smith 1992). The joint correlation analysis can be extended to correlate all orders of ISIs, called recurrence plot analysis (Aihara 1994; Eckmann et al. 1987; Kaluzny and Tarnecki 1993; Mayer-Kress and Hubler 1989; Shelhamer 1997). Note that these analyses can be applied to the same set of data with different interpretations, either in terms of stochastic theories or in terms of nonlinear dynamics in relation to deterministic chaos theories. Regardless of the differences in interpretations, these bivariate correlation analyses essentially correlate two shifted, dependent, random variables.

In this paper, we design and describe an analysis that reveals the sequential changes in firing intervals within a short pattern of consecutive spikes rather than analyzing the pattern itself. Instead of characterizing the past firing history in terms of the ISIs, τ_n, (as in most time-series analyses), we use the interspike-interval differences (ISIDs), $\Delta\tau_n$, as the random variable (Fitzurka 1996). An ISID is defined as the time difference between consecutive ISIs (i.e., $\Delta\tau_n = \tau_n - \tau_{n-1}$). This ISID variable is chosen specifically because it quantifies changes in the consecutive ISIs; positive for increasing ISIs and negative for decreasing ISIs. By determining the serial dependence relationship between these consecutive ISIDs, the local trend that we seek will ultimately be revealed. We call this technique joint-ISID (JISID) analysis (Fitzurka and Tam 1994) since it provides a joint probability density function (pdf) of the ISID pair ($\Delta\tau_n$, $\Delta\tau_{n+1}$) from which the changes in conditional pdf and transition probability matrix of a Markov process or other dependent process can be obtained. A similar analysis called 'first-order variability diagram' was employed by Babloyantz and Maurer (1996) and Maurer et al. (1997) to study the chaotic dynamics of the periodicity in cardiac rhythms. They examined the variability of deviations from regularity of the periodic pacemaker activity in the arrhythmic heart, which provided some indications of the deterministic nature of these cycles not revealed by traditional Fourier analyses (e.g., Rosenberg et al. 1989). In contrast, we derived the JISID analysis from stochastic process theories, quantifying the serial transition probabilities based on the changes of a neuron's past firing histories (Fitzurka and Tam 1995a). The statistical distributions are specifically sought so that the unknown pdf of a neuron recorded experimentally can be obtained statistically, while such statistics are not sought by other similar nonlinear analyses (Babloyantz and Destexhe 1988).

The most important aspect of this JISID analysis is that it is designed to capture firing patterns that have similar incremental changes, independent of the timescales of the ISIs (or firing rate), so that they can be classified as having the same tendency for changes, or similar trends. We shall show that the trends identified by this analysis can capture various permutations of 4-spike patterns, including periodic and aperiodic, regular and irregular, random and nonrandom patterns. Thus, our analysis is not necessarily limited to identifying the periodicity of repeated patterns or the variability of deviations from the fundamental period of cyclical patterns.

As a final note, this JISID analysis is limited to detecting the serial correlation of spike firing within a single spike train in an individual neuron. Analyses detecting the serial correlation (or temporal correlation) between the spikes of different neurons can be found elsewhere (e.g., Fitzurka and Tam 1997; Gerstein and Perkel 1972; Perkel et al. 1967b, 1975; Tam et al. 1988).

2 Methods

As discussed, this JISID analysis is similar to the traditional JISI analysis, except that ISIDs are used as the random variables instead of ISIs. Specifically, the serial correlation between two consecutive ISIDs (spanning three consecutive ISIs) is examined and quantified (Fitzurka and Tam 1995b), instead of between two consecutive ISIs (Rodieck et al. 1962). In this way, the serially dependent firing relationship spanning three (as

opposed to two) consecutive intervals can be statistically quantified.

2.1 Theoretical description

Let a spike train, $x(t)$ (Fig. 1) with a total of N spikes be represented by an n-tuple, $(t_1, t_2, \ldots, t_n)$, where t_n denotes the time of occurrence of the nth spike. An n-tuple is an ordered list of n variables. Alternatively, the spike train can be defined as

$$x(t) = \sum_{n=1}^{n=N} \delta(t - t_n) \tag{1}$$

where $\delta(t)$ denotes the Dirac delta function. The first-order ISI is defined as the time difference between two consecutive spikes. Note that there are two ISIs adjacent to a reference spike. The ISI preceding the nth reference spike (the pre-ISI, τ_n) is defined as

$$\tau_n = t_n - t_{n-1} \tag{2}$$

(see Fig. 1A) and the ISI succeeding the nth reference spike (the post-ISI, τ_{n+1}) is defined as

$$\tau_{n+1} = t_{n+1} - t_n \tag{3}$$

Generalizing this, the jth order ISI with respect to the nth spike is defined as

$$\tau_n^{(j)} = t_n - t_{n-j} \tag{4}$$

Similarly, an ISID is defined as the difference between consecutive ISIs (see Fig. 1B). The ISID preceding the nth reference spike (the pre-ISID, $\Delta\tau_n$) is defined as

$$\Delta\tau_n = \tau_n - \tau_{n-1} = t_n - 2t_{n-1} + t_{n-2} \tag{5}$$

which reflects the difference between the nth and $(n-1)$th ISI. Note that the time interval spanned by the ISID includes three spikes (see Fig. 1B), thus encapsulating a 3-spike pattern represented by a 3-tuple, (t_{n-2}, t_{n-1}, t_n). The ISID subsequent to the nth reference spike (the post-ISID, $\Delta\tau_{n+1}$) is defined as

$$\Delta\tau_{n+1} = \tau_{n+1} - \tau_n = t_{n+1} - 2t_n + t_{n-1} \tag{6}$$

Although the ISID spans two ISIs, (5) is not the same as the second-order ISI ($\Delta\tau_n \neq \tau_n^{(2)} = t_n - t_{n-2}$). Thus, the statistical analysis using this random variable, $\Delta\tau_n$, is not a simple extension of the JISI analysis using the second-order ISIs, $\tau_n^{(2)}$, as the random variable.

Statistics using the ISID, $\Delta\tau_n$, as the random variable are given below. The ISID distribution, denoted by $I(\Delta\tau)$, is represented by

$$I(\Delta\tau) = \sum_{n=3}^{N} \delta(\Delta\tau_n - \Delta\tau) = \sum_{n=3}^{N} \delta(t_n - 2t_{n-1} + t_{n-2} - \Delta\tau) \tag{7}$$

This statistical distribution provides an indicator of the changes in ISIs with respect to the reference spike, with positive ISIDs indicating a lengthening in the next ISI, and negative ISIDs representing a shortening in the next ISI relative to the previous ISI. This simple univariate ISID statistic essentially characterizes the local trend of a 3-spike pattern.

The firing trend analysis to be introduced in this paper goes beyond this simple statistical analysis of ISIDs. The focus of the analysis is on quantifying the serial relationship of the 4-spike patterns evolving over time. This 4-spike trend is characterized by correlating two consecutive 3-spike patterns (sequentially shifted by a spike relative to each other). Specifically, the serial dependence of ISIDs is characterized by a statistical JISID distribution, similar to the characterization of the serial dependence of ISIs as quantified by the statistical JISI distribution in the JISI analysis. The JISID distribution, $J(\Delta\tau_1, \Delta\tau_2)$, is given by

$$J(\Delta\tau_1, \Delta\tau_2) = \sum_{n=4}^{N} \delta(\Delta\tau_n - \Delta\tau_1)\delta(\Delta\tau_{n+1} - \Delta\tau_2) \tag{8}$$

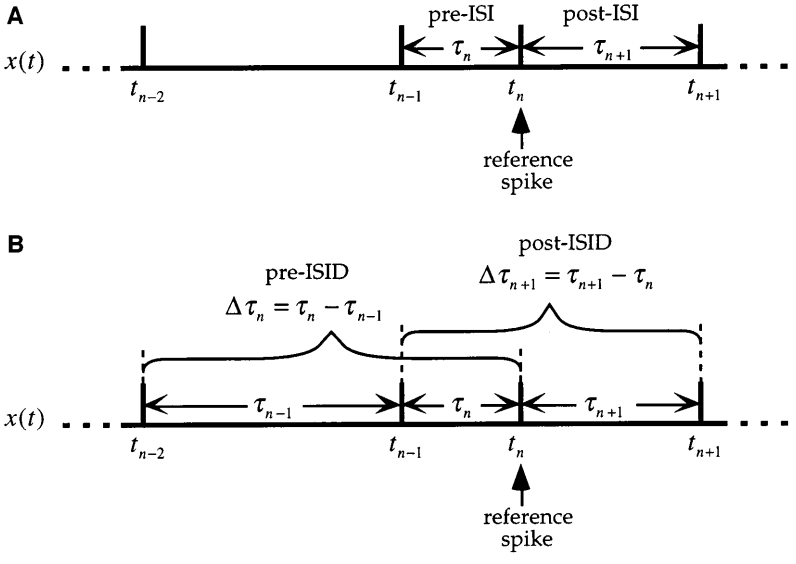

Fig. 1. Schematic diagram of a spike train showing the times of occurrence of the spikes in relation to (**A**) the interspike intervals (ISIs) and (**B**) the interspike interval differences (ISIDs)

A JISID 'scatter plot' can be constructed by plotting $(\Delta\tau_n, \Delta\tau_{n+1})$ as a point representing the (x, y) coordinate in the JISID plot for all spikes $(\forall n)$ in the spike train. That is, a scatter plot is produced by plotting $(\Delta\tau_n, \Delta\tau_{n+1})$ formed by the pre- and post-ISIDs relative to the nth reference spike for each spike used in turn as the reference spike (see Fig. 1B). Thus, each spike is represented by a point in the JISID plot, and the local trend is identified by the quadrant in which the point is located (see Sect. 3 for details). The statistical distribution of these points gives the joint distribution of (8) sought in the analysis for revealing whether there is any serial dependence between the consecutive ISIDs (i.e., with respect to consecutive changes in spike firing intervals). Normalizing (8) gives a statistical estimation of the joint pdf,

$$j(\Delta\tau_1, \Delta\tau_2) = \frac{\sum_{n=4}^{N} \delta(\Delta\tau_n - \Delta\tau_1)\delta(\Delta\tau_{n+1} - \Delta\tau_2)}{N-4} \tag{9}$$

and the conditional pdf representing the transition probability of the ISIDs is given by

$$\begin{aligned} p(\Delta\tau_2|\Delta\tau_1) &= \frac{p(\Delta\tau_1 \cap \Delta\tau_2)}{p(\Delta\tau_1)} \\ &= \frac{\sum_{n=4}^{N} \delta(\Delta\tau_n - \Delta\tau_1)\delta(\Delta\tau_{n+1} - \Delta\tau_2)}{\sum_{n=4}^{N} \delta(\Delta\tau_n - \Delta\tau_1)} \end{aligned} \tag{10}$$

Although this conditional pdf is informative in providing the transition probability (matrix) for a serially dependent process, most similar analyses in the literature plot the joint pdf instead of the conditional pdf. Traditionally, the joint probabilities are also given in a transition matrix form, while the joint distribution of the individual points are plotted in the JISI scatter plots (Rodieck et al. 1962). The main advantage of plotting the joint pdf scatter plot is to provide visualization of the exact (x, y) coordinate of the points in the plot for identifying the trends of the 4-spike patterns (see Sect. 3).

In addition to the scatter plot, a trajectory plot tracing the sequential points in the JISID analysis can be constructed by connecting the points between the nth and $(n+1)$th reference spikes, as in other interval return maps. This reveals explicitly the time evolution sequence of JISID pairs extending the analysis to establishing the relationship of a 5-spike sequence. We call this the 'serial-JISID plot' (Fitzurka and Tam 1995a).

2.2 Simulation and experimental methods

We will first analyze simulated spike trains generated with specific known spike-generating pdf's specifically to illustrate that the analysis indeed detects and identifies these specific trends. The spike trains of all simulated neurons (A-G, I-J) are generated with Gaussian-varied ISIs, with the exception of the Poisson neuron (H). The Gaussian variance at each spike is proportional to the value of the ISI preceding that spike for neurons A-G, and constant for neurons I and J. The analyses are then applied to spike trains recorded from biological neurons whose firing trends are not known a priori so that the results of these analyses can be compared and demonstrated to reveal and identify the unknown trends.

The biological neurons used in the analyses were cultured spinal cord neurons. Networks of neurons obtained from mouse embryos were cultured on multimicroelectrode plates according to the methodology described by Gross (1979) and Gross et al. (1977). Simultaneous extracellular recordings of action potentials were made from these neurons. The spike trains were digitized by a bank of digital signal processors (Plexon, Dallas) sampling at 40 KHz. These cultured neurons often fire spontaneously, though sometimes bicuculline was added to the network to disinhibit the activity. The data presented in this paper were recorded after the network was treated with bicuculline (60 µl, 1 mM).

3 Theoretical interpretations

3.1 Definitions of spike firing patterns and local trends

A 'temporal n-spike pattern' is defined by an ordered-list of the spike occurrence times, $(t_1, t_2, \ldots, t_n)$. This same pattern can also be represented by an ordered-list of ISIs, $(\tau_2, \tau_3, \ldots, \tau_n)$, called the 'ISI pattern.' This ISI pattern encapsulates all similar spike trains that are shifted in time by k (= constant), i.e., $(t_1 + k, t_2 + k, \ldots, t_n + k)$. It provides a time-shift invariant representation of the spike pattern independent of the actual spike occurrence times with a reduction of variables. Mathematically, all similar time-shifted spike trains, $(t_1 + k, t_2 + k, \ldots, t_n + k)$, will map into a single ISI pattern, $(\tau_2, \tau_3, \ldots, \tau_n)$. Similarly, the ordered-list of the ISIDs, $(\Delta\tau_3, \Delta\tau_4, \ldots, \Delta\tau_n)$, encapsulates all ISI trends that have similar incremental changes, i.e., $(\tau_2 + k, \tau_3 + k, \ldots, \tau_n + k)$, with k being a constant. All similar increment-invariant ISI patterns, $(\tau_2 + k, \tau_3 + k, \ldots, \tau_n + k)$, will map into a single ISID trend, $(\Delta\tau_3, \Delta\tau_4, \ldots, \Delta\tau_n)$.

Alternatively, the ISI pattern, $(\tau_2, \tau_3, \ldots, \tau_n)$, can be re-written as

$$(\tau_2, \tau_3, \ldots, \tau_n) = (\tau_1 + \Delta\tau_2, \tau_2 + \Delta\tau_3, \ldots, \tau_{n-1} + \Delta\tau_n) \tag{11}$$

so that the trends encapsulated by $(\Delta\tau_3, \Delta\tau_4, \ldots, \Delta\tau_n)$ are all similar ISI patterns represented by the $(n-1)$-tuple, $(\tau_1 + \Delta\tau_2 + k, \tau_2 + \Delta\tau_3 + k, \ldots, \tau_{n-1} + \Delta\tau_n + k)$ with k as a constant. This shows that ISI patterns having similar incremental changes are considered as having a similar trend according to our definitions.

Applying these definitions to 4-spike patterns, the relationship between the pre- and post-ISIDs [plotted as a point, $(x, y) = (\Delta\tau_n, \Delta\tau_{n+1})$, graphically in the JISID plot] is essentially a 2-tuple representation of the ISID trend, $(\Delta\tau_n, \Delta\tau_{n+1})$. This (x, y) point in the JISID plot also maps to all points, $(x, y, z) =$

$(\tau_{n-1}+k, \tau_n+k, \tau_{n+1}+k)$, with similar incremental changes in a 3-dimensional JISI plot. As explained above, this 3-tuple ISI pattern, $(\tau_{n-1}+k, \tau_n+k, \tau_{n+1}+k)$, also maps into any 4-spike patterns, $(t_{n-2}+k, t_{n-1}+k, t_n+k, t_{n+1}+k)$, that are independent of the absolute spike occurrence times. Thus, a point in the conventional JISI plot describes a 3-spike pattern, while a point in the JISID plot describes a 4-spike trend. Although unconventional and sometimes restrictive with these definitions, we call these similar incremental changes in intervals within the pattern a 'trend,' conforming to the tuple notation of spike patterns.

Because there are many similar 4-spike patterns represented by an ISI 3-tuple, $(\tau_{n-1}+k, \tau_n+k, \tau_{n+1}+k)$, that correspond to the same ISID pair, $(\Delta\tau_n, \Delta\tau_{n+1})$ in the JISID plot, classification of similar spike patterns into the same trend becomes automatic by this many-to-one mapping of points from the JISI plot onto the same point in the JISID plot. The advantages of this many-to-one mapping of similar spike patterns to a firing trend are given as follows. First, similar spike patterns are implicitly classified as the same firing trend mathematically and graphically. Second, the 4-spike patterns are captured by a simpler 2-tuple representation of ISIDs rather than a 3-tuple representation of ISIs or 4-tuple representation of spike times. Third, the graphical representation dimension of a 4-spike pattern is reduced from 3D (three dimensions in the JISI plot) to 2D (two dimensions in the JISID plot).

3.2 Interpretation of different regions of the JISID scatter plot

The JISID plot, which we introduce here, can be divided into four quadrants separated by the axes, each representing different 4-spike firing trends (see Fig. 2B). The relationship between the specific changes in consecutive ISIs spanning 4 spikes are identified by the insets in Fig. 2B. Points lying within the first quadrant (i.e., $\Delta\tau_n > 0$ and $\Delta\tau_{n+1} > 0$) show that the neuron fires with monotonically increasing ISIs (i.e., $\tau_{n-1} < \tau_n < \tau_{n+1}$), indicating a 'monotonically increasing trend.' Those in the third quadrant (i.e., $\Delta\tau_n < 0$ and $\Delta\tau_{n+1} < 0$) denote monotonically decreasing ISIs (i.e., $\tau_{n-1} > \tau_n > \tau_{n+1}$), implying a 'monotonically decreasing trend.' The second quadrant (i.e., $\Delta\tau_n < 0$ and $\Delta\tau_{n+1} > 0$) indicates a transition in the ISIs, changing from long to short to long (i.e., $\tau_{n-1} > \tau_n < \tau_{n+1}$), whereas the fourth quadrant (i.e., $\Delta\tau_n > 0$ and $\Delta\tau_{n+1} < 0$) indicates the opposite transition (i.e., $\tau_{n-1} < \tau_n > \tau_{n+1}$). These are called 'transitional firing trends.' [Note that these 'transitional' firing trends refer to the reversal of monotonic trends in this paper, which is distinguished from the 'transition' probability of a Markov process].

At the origin ($\Delta\tau_n = 0$ and $\Delta\tau_{n+1} = 0$), the ISIs remain constant (i.e., $\tau_{n-1} = \tau_n = \tau_{n+1}$), indicating a 'constant trend.' Points falling along the axes represent 'ramp firing trends.' Two types of ramp trends are found along the x-axis. Points lying along the $+x$-axis represent a ramp trend with $\tau_{n-1} < \tau_n = \tau_{n+1}$ (increasing ramp trend II), while points lying along the $-x$-axis signify a ramp trend with $\tau_{n-1} > \tau_n = \tau_{n+1}$ (decreasing ramp trend I). Similarly, two other types of ramp trends are found along the y-axis. Along the y-axis ($\Delta\tau_n = 0$) the ramp trends revealed are $\tau_{n-1} = \tau_n < \tau_{n+1}$ for the $+y$ axis (increasing ramp trend I), and $\tau_{n-1} = \tau_n > \tau_{n+1}$ for the $-y$-axis (decreasing ramp trend II).

In summary, each point in this JISID scatter plot corresponds to two adjacent interval difference pairs, $(\Delta\tau_n, \Delta\tau_{n+1})$, or three adjacent intervals, $(\tau_{n-1}, \tau_n, \tau_{n+1})$, or four adjacent spikes, $(t_{n-2}, t_{n-1}, t_n, t_{n+1})$; whereas each point in the traditional JISI scatter plot (see Fig. 2 A) represents only two adjacent intervals (τ_n, τ_{n+1}), or three adjacent spikes, (t_{n-1}, t_n, t_{n+1}).

3.3 Interpretation of the serial-JISID scatter plot

The evolution of the changes in firing, or firing trends, can be further deduced from the serial-JISID plots. These consecutive changes in ISIDs are represented by the sequence of quadrants the sequential points traverse. The serial dependence of these changes is determined by visualizing within which quadrants sequential points are located with respect to each other, and the angle of the line connecting the sequential points.

4 Simulation and experimental results

4.1 Identification of unique trends based on quadrant

A spike train with a repeated 'triangularly modulated' sequence is simulated for neuron A, whose ISIs increase monotonically by a constant amount then decrease monotonically by the same constant amount. It is immediately evident that this neuron fired with four distinct trends, as seen by clusters in each quadrant (Fig. 3A). The clusters in quadrants 1 and 3 represent the monotonically increasing and decreasing firing trends, respectively, while the clusters in quadrants 2 and 4 represent the long-short-long and short-long-short transition firing trends (refer to Fig. 2B).

Comparing the JISI (Fig. 3B) analysis to the JISID (Fig. 3A) analysis for this neuron (cf. Fig. 2A for interpretation), there are eight distinct clusters found as opposed to only four. Thus, there are eight distinct 3-spike patterns found by JISI analysis, yet only four distinct trends found by JISID analysis, because similar incremental patterns are classified as the same trend. For example, the four clusters (a)–(d) above the diagonal in the JISI plot represent the four proportional patterns that are captured by a single trend in the cluster (a) in quadrant 1 (monotonically increasing trend quadrant) in the JISID plot.

In constrast to neuron A, neuron B (which fires with a triangularly modulated 'sawtooth-shaped' repeated monotonically increasing sequence) has one cluster in quadrant 1 (monotonically increasing trend quadrant) but no cluster in quadrant 3 (monotonically decreasing trend quadrant) of the JISID plot (Fig. 3C). Comparing

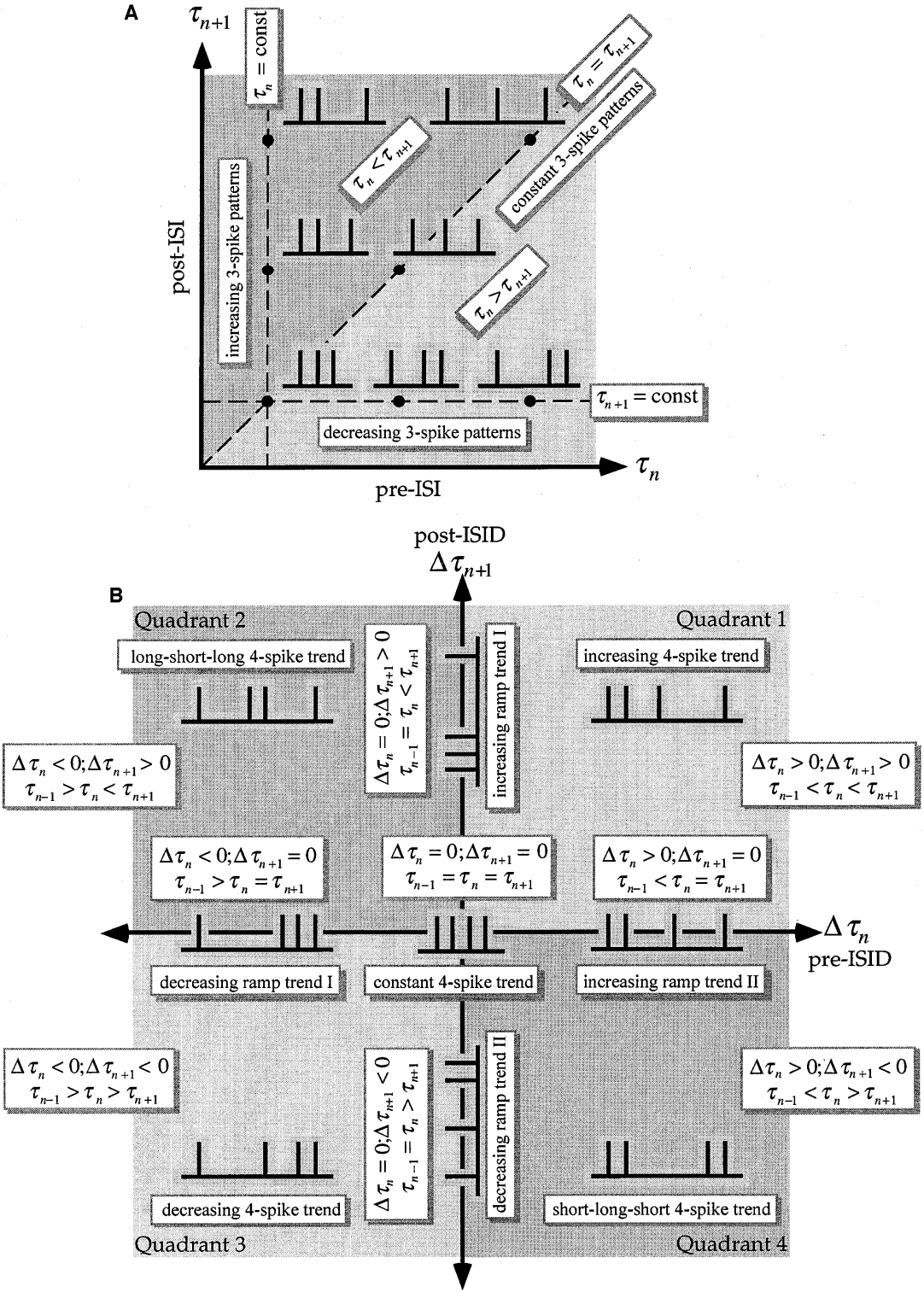

Fig. 2. Interpretation diagrams for the joint-ISI (JISI) (**A**) and joint-ISID (JISID) (**B**) scatter plots indicating the firing patterns that correspond to different regions on the plot as depicted by the *insets*

neuron C (simulated with a repeated triangularly modulated monotonically decreasing sequence) with neuron B, we see that a cluster is found in the monotonically decreasing quadrant 3 (Fig. 3E) as opposed to the monotonically increasing quadrant 1 (see Fig. 3C), which is as expected.

In summary, distinct trends are revealed by the characteristic features in the JISID plots. First, the transitional trends for these neurons are different, i.e., those for neurons B and C show more abrupt asymmetrical transitions than A. This can be deduced by comparing the proximity of the clusters to the axes in quadrants 2 and 4.

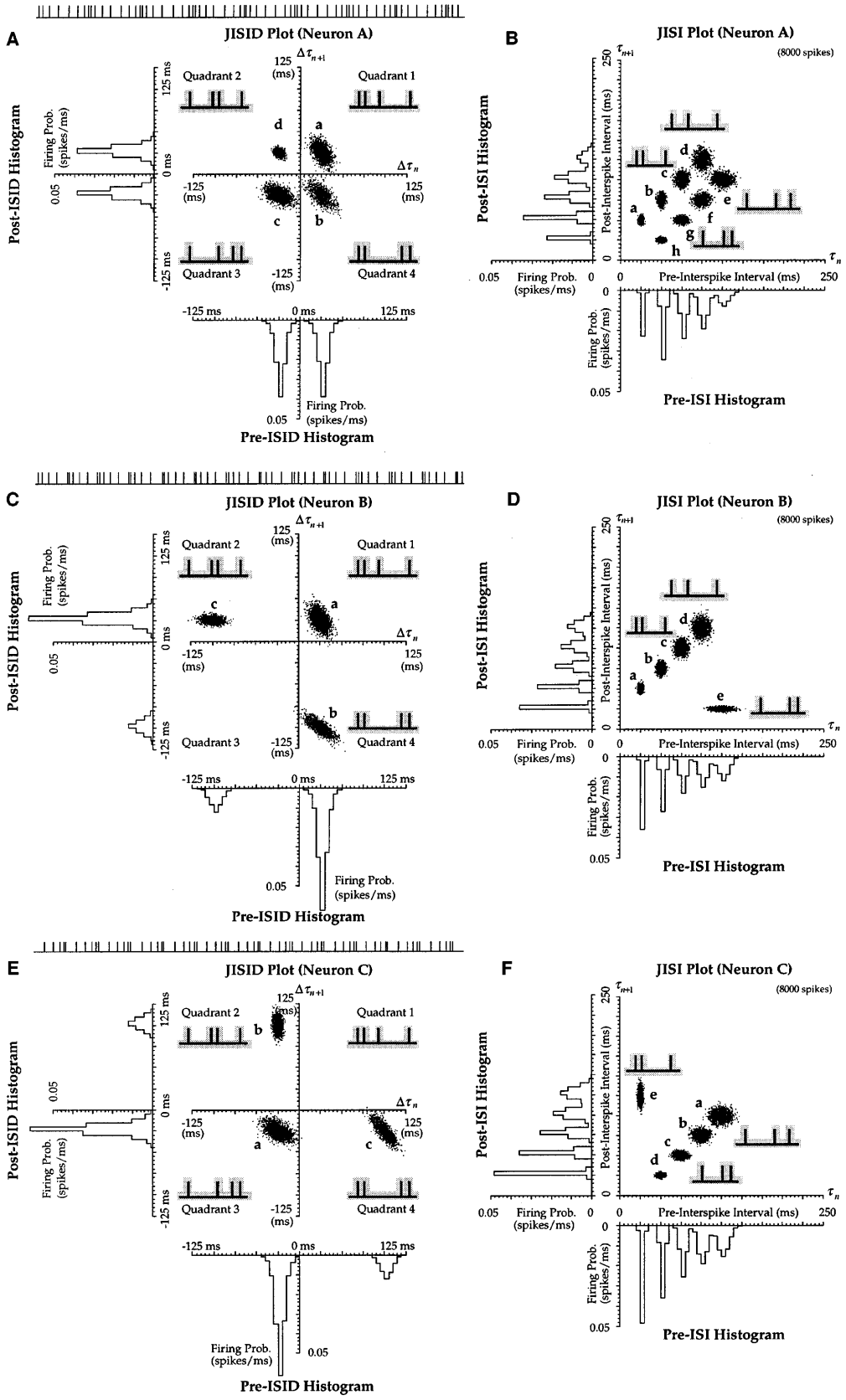

Fig. 3. JISI and JISID scatter plots for neuron A firing with triangularly modulated spike patterns (**A**, **B**), for neuron B firing with repeated increasing triangular sawtooth spike patterns (**C**, **D**), and for neuron C firing with repeated decreasing sawtooth spike patterns (**E**, **F**). A segment of the spike train is displayed above the JISID plot for each neuron. Example spike patterns corresponding to the clusters are shown as *insets*. [The histograms *underneath* and to the *left* of the JISID and JISI scatter plots represent the ISID and ISI histograms, using a 5 ms bin-width]

Second, it can be noted that some neurons do not necessarily fire with all four trends classified by the quadrants. Third, the JISID analysis did indeed identify and classify similar incremental patterns as the same trend for all these neurons. In particular, the similar proportional 4-spike patterns that belong to the same monotonic trends are identified by a single cluster in the JISID plot that corresponds to multiple clusters aligned parallel to the diagonal in the corresponding JISI plots.

When these bivariate joint interval (JISI and JISID) analyses are compared with the univariate (ISI) analysis, the distributions of points in the JISI scatter plots are not symmetrical about the central diagonal (see Fig. 3D, F); however, the pre-ISI and post-ISI histograms are the same, as expected by definition. In fact, these ISI histograms can be considered as histograms constructed by collapsing (summing) all points in the JISI plot onto the x- or y-axis, respectively. Furthermore, the ISID histograms alone do not reveal the specific 4-spike trends that JISID plots reveal, similar to the fact that ISI histograms do not uncover the specific 3-spike patterns that JISI plots uncover. Finally, the ISI distributions (see Fig. 3B, D, F) for all three neurons are similar (and, in fact, almost identical for B and C), yet the JISI and JISID distributions are distinctly different. This shows that bivariate analyses (such as JISI and JISID) are essential in distinguishing the differences in trends and patterns unique to each neuron.

4.2 Detection of multiple trends in sinusoidally modulated firing

The JISID plot (Fig. 4A) of neuron D (firing with sinusoidally varying ISIs) shows that there are points in all four quadrants. All four main types of firing trends are represented. For comparison, the clusters for the sinusoidally modulated neuron, D, outline an elliptical ring (Fig. 4A,C), whereas the clusters for the triangularly modulated firing neuron, A, outline the corners of a rectangle (Fig. 3B). This reveals the differences between specific abrupt and smooth trends, as in the triangular and sinusoidal cases, respectively.

Figure 4C, D displays the JISID and JISI histograms representing the 3D topographical profile of the joint pdf's. The transition probabilities at various intervals are represented by the peaks of the histograms. The transition probability is zero except for the time intervals outlined by the elliptical 'ring' for both JISI and JISID pdf's (Fig. 4C,D). This is consistent with the fact that differentiating a sine function gives a cosine function, and that the sine and cosine functions are essentially sinusoidally modulating waveforms (both represented as an ellipse in a phase plane). Thus, JISID analysis is analogous to the 'differentiation' of the JISI analysis. It is clear that the size of the 'spread' of points about each cluster simply reflects the proportional Gaussian variance used at each firing interval and does not necessarily imply higher firing probabilities. The merging of the clusters can be considered more an advantage than a disadvantage because the joint pdf with a merged elliptical outline is characteristic of sinusoidally modulated firing trends. This illustrates that cluster analysis is not needed to identify and/or separate the individual clusters in the JISI or JISID scatter plots.

4.3 Detection of transitional trends in burst firing

The JISID scatter plot for a bursting neuron, D (Fig. 5A), reveals the burst-onset trend by cluster (d) along the $-x$-axes; the intraburst (constant) trend by cluster (a); the burst-offset trend by cluster (b) along the $+y$-axis; and the transitional trend from end-of-burst to beginning-of-next-burst by cluster (c) along the antidiagonal ($-45°$ line). These precise firing trends (burst-onset, burst-offset, and transitional trends) are clearly revealed by the specific quadrants and axes in which the clusters are located in the JISID plot. The symmetry along the antidiagonal implies that this neuron enters into a burst-firing sequence the same way as it terminates its burst-firing.

Comparing the JISI plot (Fig. 5B) with the JISID scatter plot (Fig. 5A), incidentally, there are more clusters found in the latter (i.e., four clusters vs three). This is because there are more types of changes in firing than the types of firing patterns for this neuron. It is also important to recognize the correspondence between the trajectory lines in a serial-JISI plot (Fig. 5D) and the clusters in a JISID scatter plot (Fig. 5A). For example, the vertical trajectory from (a) to (b) in the serial-JISI plot (Fig. 5D) represents the same 4-spike trend as the cluster (b) in the JISID scatter plot (Fig. 5A). The trend unidentified in the JISI plot is the constant trend found explicitly in cluster (a) in the JISID scatter plot (Fig. 5A). This degeneracy is due to the fact that no distinct trajectory lines are drawn when the spike patterns remain relatively constant within cluster (a) in the JISI plot (Fig. 5D).

Finally, the serial-JISID plot (Fig. 5C) can provide an additional level of description to the JISID plot similarly to the serial-JISI plot. By tracing sequential points, the serial-JISID plot reveals the sequence in which the 4-spike trends are changing. Thus, 5-spike trends can be recovered from the trajectory trace in the serial-JISID plot, as indicated by the 5-spike insets in the figure. It is immediately evident that an outline of a 'southeasterly pointing arrowhead' characterizes the four different 5-spike trends revealed by the serial-JISID analysis. This arrowhead trajectory is characteristic of burst-firing trends traced in a clockwise fashion as shown in Fig. 5C. It will be shown below that this arrowhead trajectory is also a characteristic of other irregular, nonperiodic burst-patterns.

4.4 Detection of transitional trends in arrhythmic pacemaker firing

Next, we will use our JISID analysis to determine the trends characteristic of a pacemaker neuron, F, that occasionally skips periods (25% failure probability).

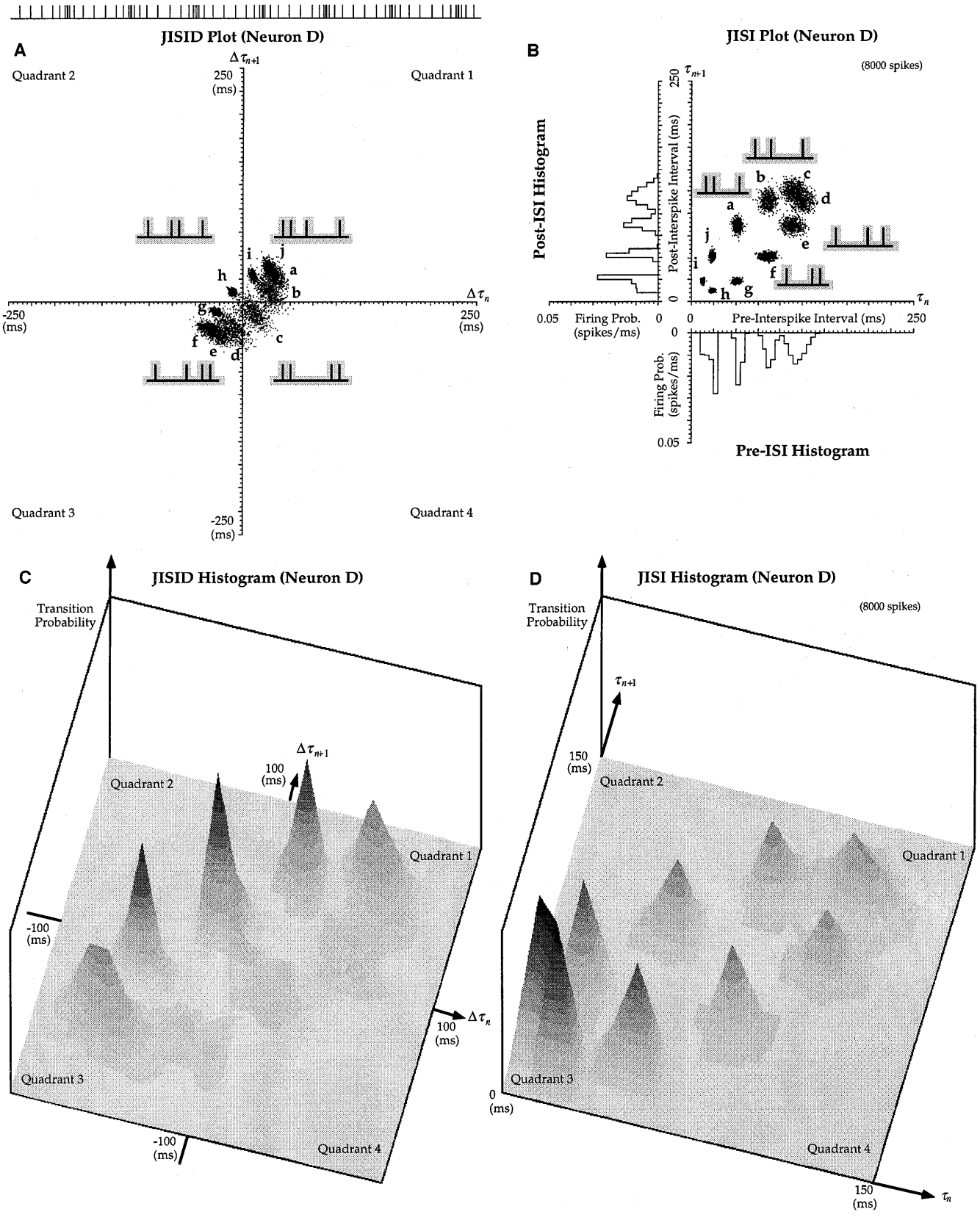

Fig. 4. JISID (**A**) and JISI (**B**) scatter plots for the sinusoidally modulated firing neuron D. Three-dimensional JISID (**C**) and JISI (**D**) histograms show the joint (transition) probabilities of 4-spike firing trends and 3-spike firing patterns, respectively

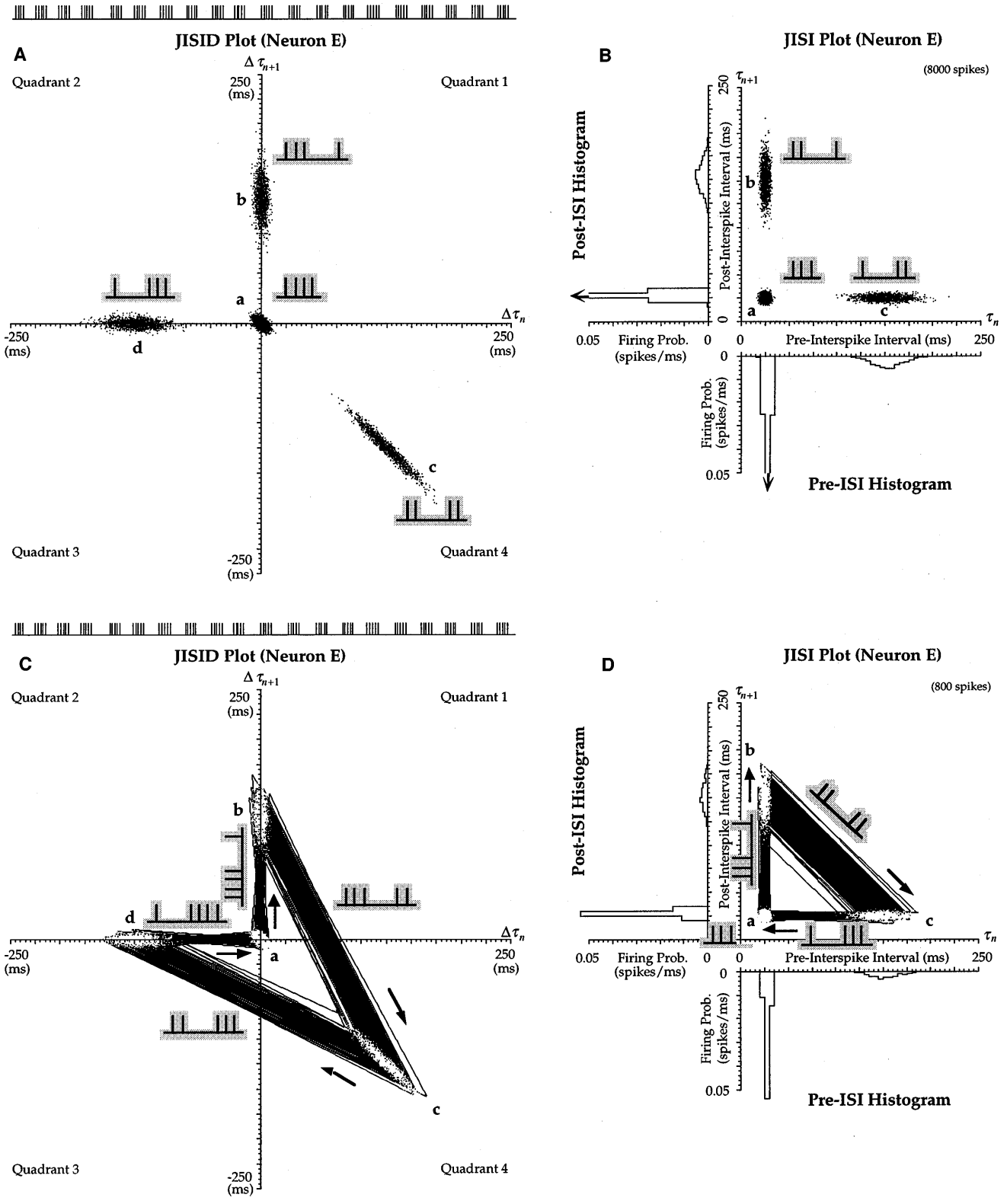

Fig. 5. JISID (**A**) and JISI (**B**) scatter plots for the burst firing neuron E. Serial-JISID (**C**) and serial-JISI (**D**) scatter plots for a short segment of the bursting data. [*Arrows* shown in the pre-ISI and post-ISI histograms (in **B**) indicate that the amplitude of the histogram bar extends beyond the current scale of the graph] [Arrows shown in the serial-JISID and serial JISI plots (in **C** and **D**) indicate the clockwise direction of sequential evolution of points]

[This arrhythmicity is sometimes called 'skipping' by Longtin and Hinter (1996) and Segundo et al. (1991).] A central cluster at the origin in the JISID plot (Fig. 6A) indicates a constant pacemaking trend. The other secondary outlying clusters at integral multiples of ISIDs reveal the various trends resulting from the skipped

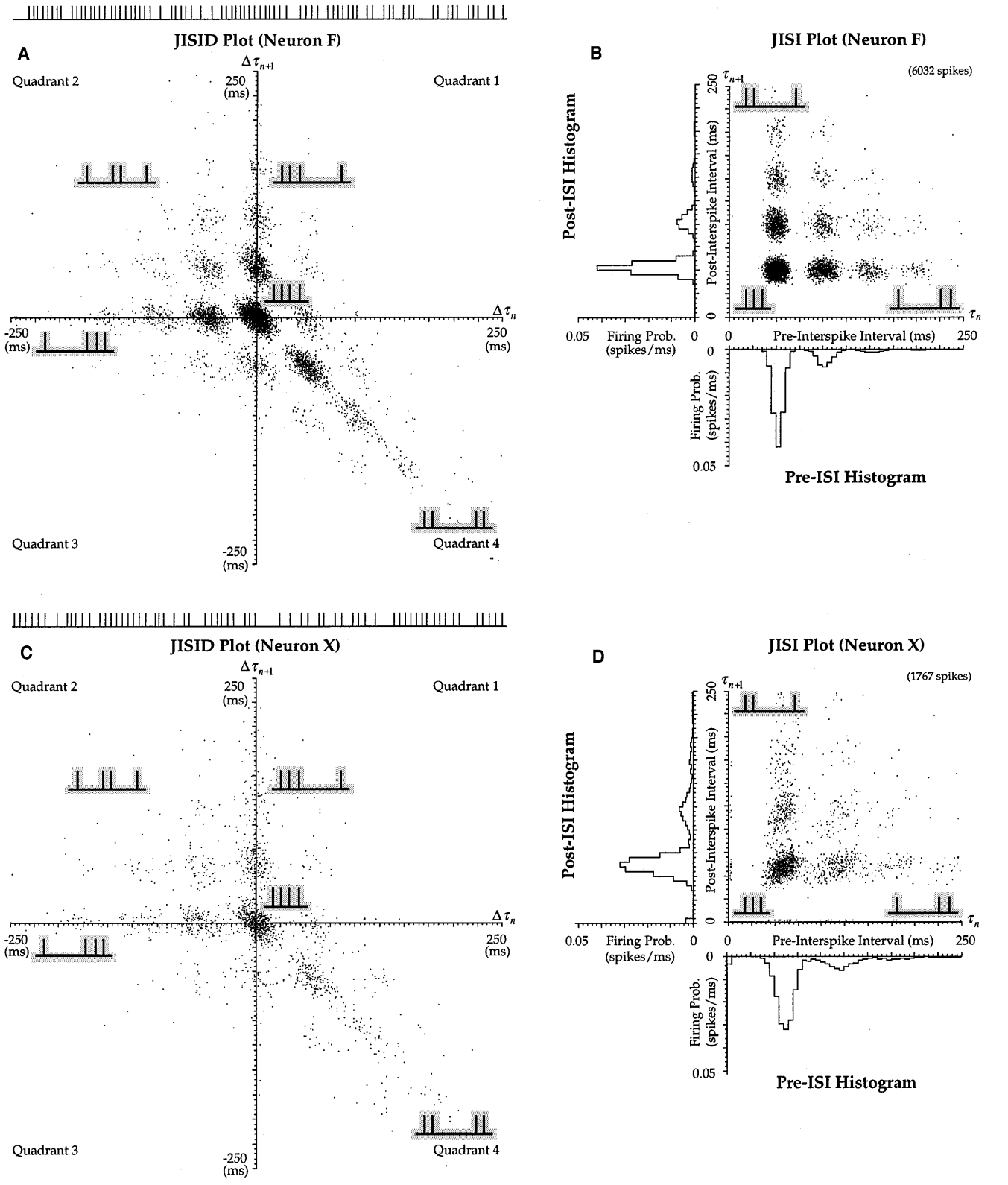

Fig. 6. JISID (**A**) and JISI (**B**) scatter plots for the arrhythmic pacemaker neuron F. JISID (**C**) and JISI (**D**) scatter plots for biological neuron X

periods. This characterizes the trends for an arrhythmic pacemaker neuron since there is a predominance of a fundamental ISI with only sporadic 'drop-outs' in firing, creating other sporadically changing trends. Another interesting feature is the transitional trend characteristic of a burst-like firing neuron uncovered by the clusters lying within a 'southeasterly pointing arrowhead' for this arrhythmic pacemaker neuron F (cf. Figs. 5A and 6A).

Figure 6C,D shows the JISID and JISI scatter plots for a biological neuron, X. The clusters of points for this

neuron are similar to neuron F (cf. Fig. 6A,C). This shows that the JISID analysis does indeed reveal the transitional trends that are characteristic of an arrhythmic pacemaker neuron, not only in a simulated neuron but also in a real biological neuron, without any a priori knowledge of the firing trends regarding rhythmicity.

4.5 Detection of transitional trends in alternating biperiodic firing

A biperiodic neuron, G, is simulated to alternate between two Gaussian-varied periods with occasional drop-outs (25% failure rate) in firing. It is immediately evident from the JISID plot (Fig. 7A) that the majority of points fall within two clusters in quadrants 2 and 4, i.e., the long-short-long transition and the short-long-short transition quadrants. This suggests that the neuron tends to fire with transitional trends most of the time, revealing the two alternating trends. The secondary clusters seen at the origin and on the $+x$- and $-y$-axes are a result of the neuron failing to follow strictly alternating firing, consistent with the simulation parameters. [Note that this type of biperiodic firing trend is not necessarily the same as 'doublet' firing because a neuron can fire doublets periodically (as in this example) or it can fire doublets randomly (which is not biperiodic). A different spike train analysis can be used to extract the doublet firings characteristics in relation to temporal integration (Tam 1998). It will be shown below (see Sect. 4.7, Fig. 9) that this JISID analysis can actually be used to distinguish spike trends that are repeated either periodically or randomly.]

Comparing neurons E and G, it is obvious from the ISI histograms (see Figs. 5B and 7B) that both neurons fired primarily with a short period and occasionally a long period, yet these histograms do not distinguish the difference between the burst firing (neuron E) and the alternating biperiodic firing (neuron G), nor do they distinguish the different transitional trends uncovered by the JISID analyses. Furthermore, clusters located in the 'southeasterly pointing arrowhead', characteristic of the bursting neuron E (Fig. 5A), are not found at the corresponding locations for neuron G (Fig. 7A) in the JISID plots. The JISID analysis clearly distinguishes the transitional trends between a bursting neuron and an alternating biperiodic neuron. This illustrates that higher-order interval serial correlation analyses, such as the JISID analysis, are needed to quantify higher-order firing characteristics.

Compared with the cultured neuron, Y, in the same network (Fig. 7C,D), clusters are found similar to neuron G. Note that although these two neurons fire with spike patterns in different time-scales, the difference in time-scales of spike patterns (and mean firing rates) between these two neurons does not preclude the ability of the JISID analysis to extract the biperiodic trends with occasional drop-outs for both neurons. This demonstrates the robustness of the JISID analysis in identifying local trends independent of the specific time-scale.

4.6 Characteristics of random firing

Next, we will examine the characteristics of a neuron, H, firing randomly with a Poisson process to provide the baseline (control) pdf needed for comparison between a neuron that fires randomly from a neuron that does not. The JISI scatter plot for this neuron (Fig. 8B) follows a 2D negative exponential distribution with dead-time in both the τ_n and the τ_{n+1} axis directions. This is consistent with the fact that if a neuron fires with an independent process, the JISI histogram (or joint pdf) is equal to the product of the pre-ISI and post-ISI histograms. This analysis also reveals Poisson-like firing trends in another spinal cord neuron, Z, (Fig. 8C,D) recorded in the same cultured network as neurons X and Y, even though we included significantly fewer spikes in the analyses for the biological neurons.

The JISID analysis for this neuron (Fig. 8A) reveals that most of the points are found to fall close to the origin, indicating that most of the time there is little change in consecutive firing intervals (refer to Fig. 2B). It is important to point out that the distribution of points does not resemble any negative exponential profiles symmetrical about the x- and y-axes, as if the JISI plot (Fig. B) were reproduced in all four quadrants. Instead, the topographical profile of the JISID plot outlines a south-easterly pointing arrowhead (Fig. 8A). This is consistent with the fact that a Poisson neuron's firing often resembles a 'burstlike' pattern since the probability of a short ISI occurrence is much greater than a longer ISI occurrence (see ISI histogram of Fig. 8B), producing a pseudo-burstlike pattern. Note also that the refractory period is reflected in the absence of points close to the axes in the JISI plot, but no such absence is found at the origin in the JISID plot because the dead-time is theoretically 'subtracted' in the ISIDs.

This 'arrowhead' distribution for a Poisson neuron further illustrates that JISID analysis is not merely a simple collapse of a 3D JISI plot (not shown) into a 2D JISID plot. By definition, the joint pdf of a 3D JISI plot should be equal to the product of three identical pdf's of the ISI plots for an independent process. However, the distribution in the JISID plot for a Poisson process (Fig. 8A) does not resemble the product of the pre- and post-ISID distributions (Fig. 8A) as if the pre- and post-ISIDs are independent, nor does it resemble the symmetrical distribution about the x- and y-axes, as if the JISI plot (Fig. 8B) were reproduced in all four quadrants. This is because the pre- and post-ISIDs are not independent variables (as discussed in Sect. 1) by definition from (5) and (6). Thus, the JISID analysis is not equivalent to a 3D JISI analysis projected onto a 2D plane.

4.7 Detection of the same trends independent of whether they repeat randomly or periodically

Lastly, we will illustrate the ability of the JISID analysis to detect the same firing trends independent of whether

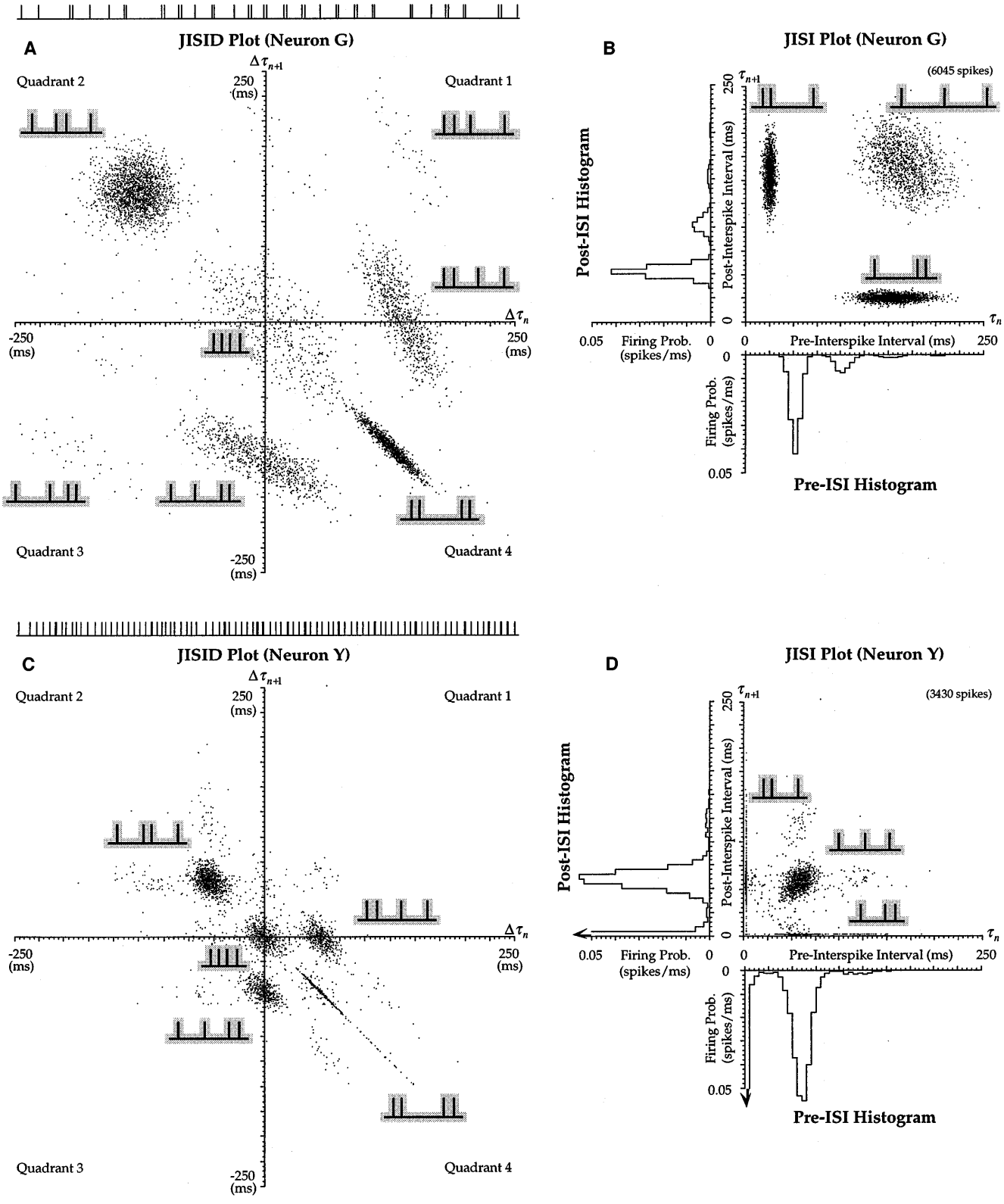

Fig. 7. JISID (**A**) and JISI (**B**) scatter plots for the alternating biperiodic neuron G. JISID (**C**) and JISI (**D**) scatter plots for biological neuron Y

they repeat randomly or periodically. This is of particular importance in detecting and identifying any arbitrary spike patterns that may be encoded by neurons. We simulated an arbitrary sequence of spikes representing a particular 4-spike pattern encoded by neurons I and J. The Gaussian-modulated 4-spike pattern selected is represented by the mean ISI 3-tuple (19, 31, 73 ms), with prime numbers for the ISIs to avoid periodicity

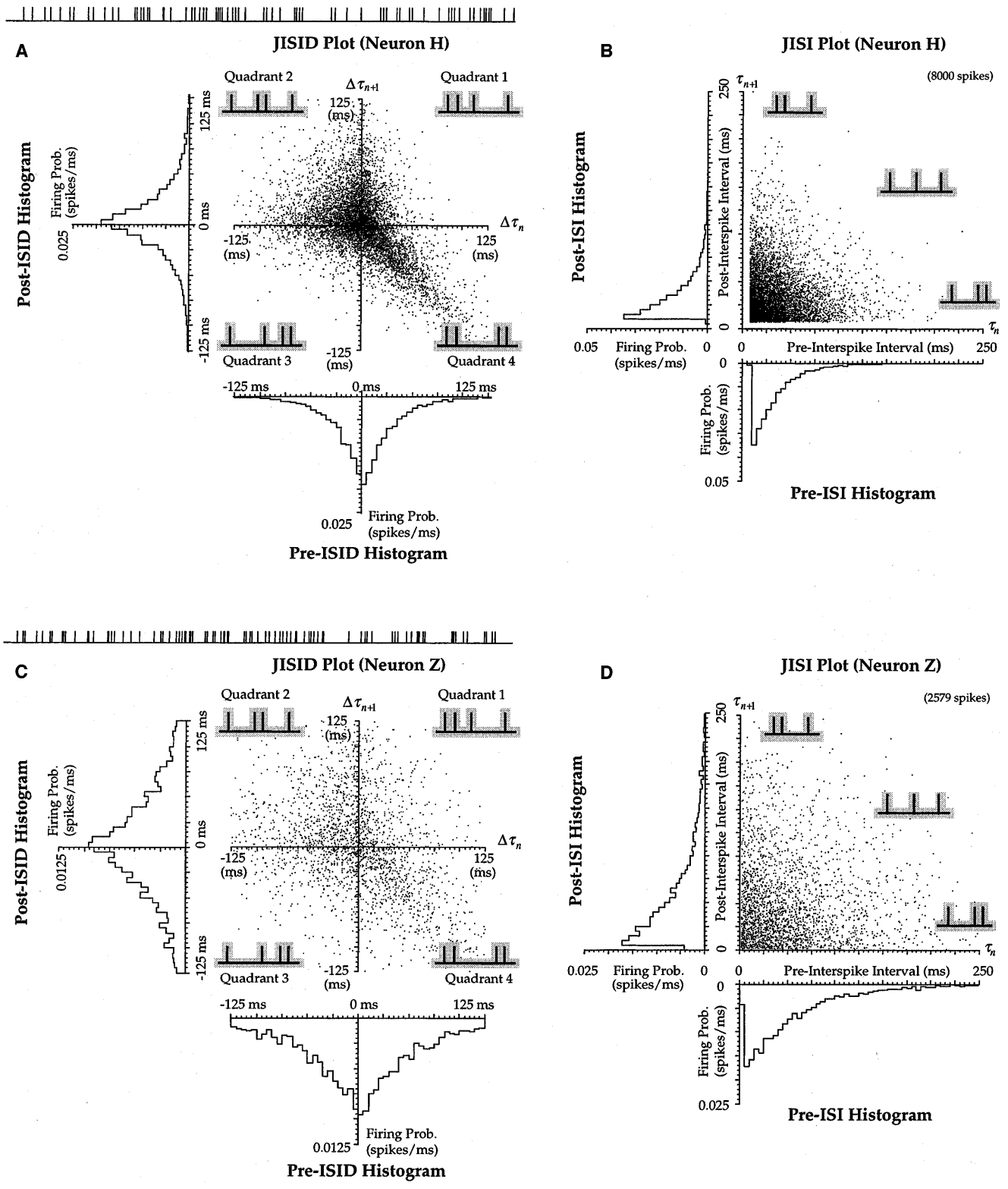

Fig. 8. JISID (**A**) and JISI (**B**) scatter plots for the Poisson neuron H. JISID (**C**) and JISI (**D**) scatter plots for biological neuron Z

within the pattern itself. Both neurons I and J fire with this same 4-spike pattern, except that neuron I repeats this pattern periodically with a mean interburst period of 179 ms (another prime number), while neuron J repeats this pattern randomly.

The JISID plots (Fig. 9A,C) for these neurons clearly show a centrally located cluster (a) that corresponds to the trend of the 4-spike burst pattern for both neurons as predicted. The outlying clusters (b), (c), and (d) in Fig. 9A represent the other repeated trends trailing and

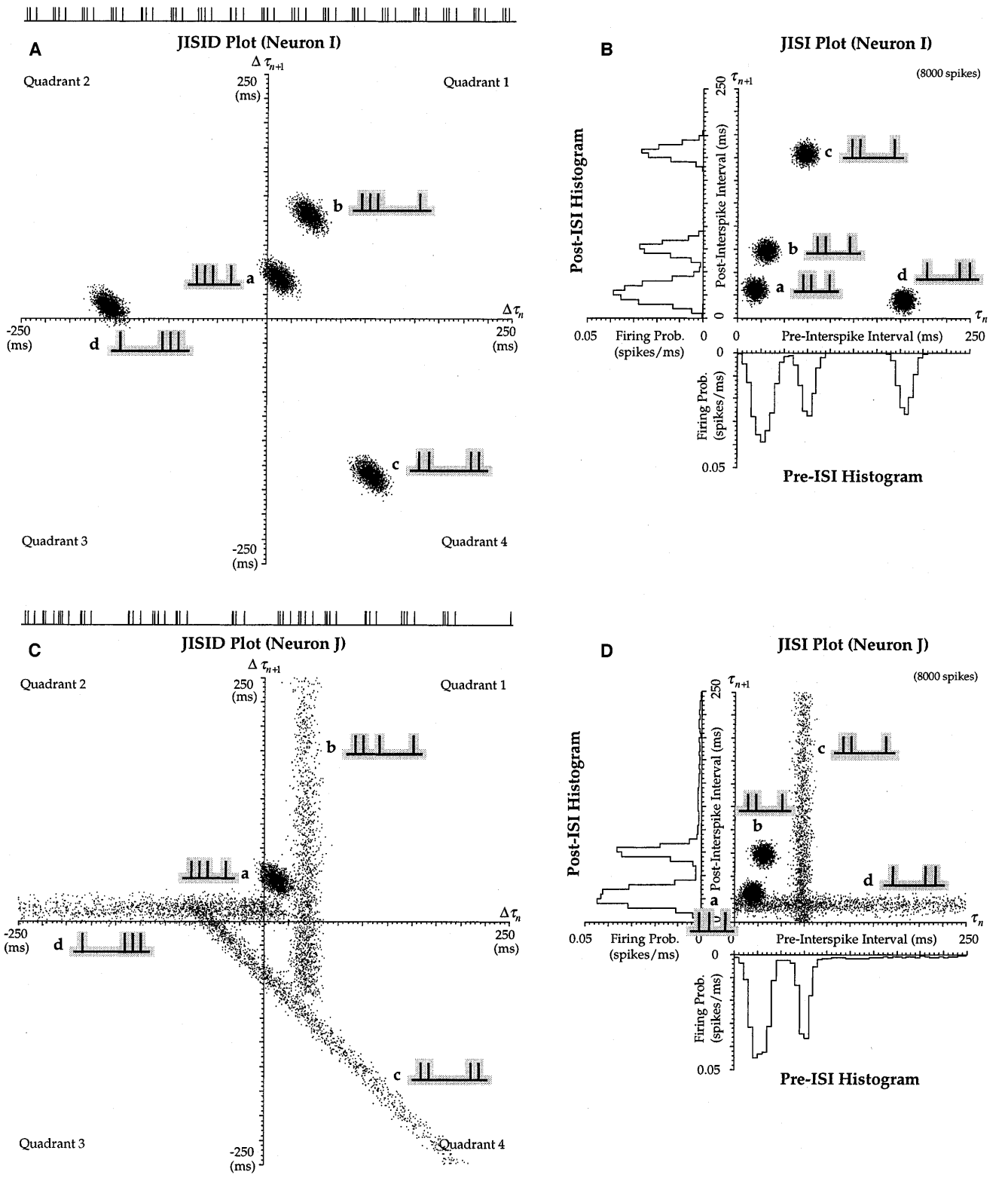

Fig. 9. JISID (**A**) and JISI (**B**) scatter plots for neuron I firing with a periodically repeated 4-spike burst pattern. JISID (**C**) and JISI (**D**) scatter plots for neuron J firing with the same 4-spike pattern as neuron I except that the patterns are repeated randomly

leading to the burst pattern, consistent with the fact that neuron I repeats this pattern periodically. Compared with Fig. 9C, three diffuse bands of points are found surrounding the central cluster (a) in Fig. 9C, indicative of the variety of trends leading to or trailing this repeated 4-spike pattern. It is important to notice that points are not distributed uniformly throughout the JISID plot (Fig. 9C) nor dispersed with a distribution

similar to that of the Poisson neuron H (see Fig. 8A), even though neuron J randomly repeats the 4-spike pattern. Most importantly, based on the JISID plot, we can infer that it fires most often with a single repeated trend as indicated by the central peak cluster (a), and that this spike sequence repeats randomly as indicated by the radiating bands, unlike neuron and (cf. Figs. 8A and 9A).

Lastly, clusters (and bands) of points are often found to 'cross' the quadrant boundaries. For instance, cluster (a), representing the 4-spike pattern (19, 31, 73 ms), crosses the boundary of quadrants 1 and 2 for neurons I and J (Figs. 9A,C). Based on the theoretical analyses described above (refer to Fig. 2B), this 'switching' in trend actually represents a 'gradual' transition from one type of trend to another, rather than an 'abrupt' transition . In fact, if the Gaussian variance of the ISIs for neuron I is reduced, the clusters would not cross the quadrant boundaries. This demonstrates that quadrant boundary crossing is not necessarily indicative of abrupt switching or chaos, because the underlying spike generation process is still the same.

5 Discussion

We have demonstrated that the JISID analysis introduced in this paper can extract local trends in firing both theoretically and experimentally. This method is shown to extract local firing trends defined by sequential changes in ISIs. This local trend provides a description of the serial dependence of spike firing. We have extended the traditional JISI serial dependence analysis to include changes within these intervals. Using this JISID analysis allows us to capture different incremental changes in spike patterns that have similar trends. The local trend, as defined and discussed in this paper, characterizes the spike patterns that include fewer than six spikes.

One of the advantages of this analysis is the graphical identification of the trends by the quadrants. The nature of the trend, representing how the spike firings are changing, is explicitly represented in the graph. Specific trends are identified by the location of points in a quadrant, while others are revealed by the proximity of points to the axis or origin.

Another advantage of this analysis is that an additional order of the prior history is captured implicitly. Although this analysis is not the only correlation analysis that correlates higher-order ISIs, it does differ fundamentally in many respects. First, while most other correlation analyses characterize the dependence relationship in terms of the spike occurrence intervals, the JISID analysis describes the changes in these time intervals. The changes in the past history that affect the spike firing are captured by two consecutive ISIDs (i.e., three consecutive ISIs). Second, while autocorrelation recurrence analysis describes all higher-order ISIs (Kaluzny and Tarnecki 1993; Shelhamer 1997), JISID analysis extracts only the lower-order ISIs. We specifically select the lowest-order ISIs for the analysis because we want to find out whether the lowest-order ISIs are sufficient to quantify the sequential changes in spike firing. Furthermore, the pdf's of the lower-order ISIs are often 'buried' by the pdf's of the higher-order ISIs in autocorrelograms when all orders of ISIs are plotted on the same graph. Finally, this analysis is different from the one that displays the jth order ISI difference at each nth spike relative to the shifted $(n+j)$th spike (Segundo et al. 1995).

Although this JISID analysis plots the serial relationships of the lower-order ISIs, the relationship in the next higher order can also be revealed by connecting sequential points in the JISID plot as is traditionally done with other return map analyses. The resulting 'trajectory' reflects the evolution of trends and identifies the sequential trends by tracing the different quadrants the points traverse (i.e., it shows how trends can change from one type to another). A higher-order serial dependence, if it exists, can be deduced by these trajectory plots.

Another advantage is the reduction of dimensions (from 3D to 2D) needed to represent these sequential changes or firing trends, or a reduction from the 3-tuple $(\tau_{n-1}, \tau_n, \tau_{n+1})$ to a 2-tuple $(\Delta\tau_n, \Delta\tau_{n+1})$ representation. While a 3D JISI return map has been used to represent the 3-tuple, this JISID analysis re-maps the same information onto a 2D representation differently. As noted in Sect. 4.6, such a mapping is not a simple, direct topographical projection from a 3D space onto a 2D plane.

An added advantage is that this 2-tuple measure (JISID pair) quantified by the JISID analysis represents relative changes explicitly (regardless of the time-scale of the ISIs). Since a single point in the JISID plot can map into multiple points in the 3D JISI return map, a unique trend identified by the JISID analysis cannot be equivalently represented by the 3D JISI analysis. The interpretation is that a unique trend identified by a point in the JISID analysis corresponds to a set of similar incrementally changing firing patterns, $(\tau_{n-1}+k, \tau_n+k, \tau_{n+1}+k)$, in the 3D JISI analysis. Most importantly, the classification of similar patterns into the same trend allows us to compare changes in patterns that are in different time-scales. This time-invariant method of detection of spike trends is different from the other time-invariant spike trend detection methods using a spike index employed by Tam (1996).

As a consequence of this many-to-one mapping from a 3-tuple to a 2-tuple representation (or equivalently, from 3D to 2D), multiple spike patterns are mapped into the same trend. This degeneracy precludes identification of the exact spike patterns that correspond to the same trend. However, this information representing the original ISI pattern can be recovered with a related analysis called 'first order ISID phase plane analysis' (Fitzurka and Tam 1996a), where the specific relation between the ISIs and ISIDs are retrieved by plotting a given ISID with respect to its associated ISIs. Furthermore, another higher-order serial dependence can be revealed by the 'second-order ISID phase plane analysis' (Fitzurka and Tam 1996b).

Finally, the trends revealed within the spike patterns by this JISID analysis are not limited to periodic or quasi-periodic, regular or irregular, chaotic or nonchaotic patterns. Any 4-spike pattern, in any combination or permutation, whether periodic or random, can be classified into specific trends because these trends are identified simply by the quadrant in which the point is located. The most significant contribution of this analysis is that it can be applied universally to classify any type of 4-spike firing trend regardless of its periodicity or randomness of the trends and patterns, because no a priori assumptions were made about the linearity or nonlinearity of the underlying process that generates the particular spike patterns.

Acknowledgements. This research was supported by the Office of Naval Research (ONR grant numbers N00014-93-1-0135 and N00014-94-1-0686) and the Faculty Research Grant from the University of North Texas to D.C.T.

References

Aihara K (1994) Chaos in neural response and dynamical neural network models: towards a new generation of analog computing. In: Yamaguti M (ed) Towards the harnessing of chaos. Elsevier, Amsterdam, pp 83–98

Babloyantz A, Destexhe A (1988) Is the normal heart a periodic oscillator? Biol Cybern 58:203–211

Babloyantz A, Maurer P (1996) A graphical representation of local correlations in time series – assessment of cardiac dynamics. Phys Lett A 221:43–55

Brillinger DR (1975) Time series: data analysis and theory. Holt, Rinehart and Winston, New York

Correia MJ, Landolt JP (1977) A point process analysis of the spontaneous activity of anterior semicircular canal units in anesthetized pigeon. Biol Cybern 27:199–213

Cox DR, Lewis PAW (1966) The statistical analysis of series of events. Methuen, London

Eckmann J-P, Kamphorst SO, Ruelle D (1987) Recurrence plot of dynamical systems. Europhys Lett 4:973–977

Fitzurka MA (1996) Internal network dynamics of cultured neuronal networks: new techniques in the theory of spike train analysis. Ph.D. Dissertation, UMI, Ann Arbor, Michigan

Fitzurka MA, Tam DC (1994) A new spike train analysis technique for detecting trends in the firing patterns of neurons. Third Annual Conference on Computational Neural Systems, Monterey, CA, p 101 (abstract)

Fitzurka MA, Tam DC (1995a) A new spike train analysis technique for detecting trends in the firing patterns of neurons. In: Bower JM (ed) The neurobiology of computation. Kluwer, Boston, pp 73–78

Fitzurka MA, Tam DC (1995b) A new statistical measure for detecting trends in the firing patterns of neurons. In: Witten M, Vincent DJ (eds) Building a man in the machine: computational medicine, public health, and biotechnology. (Series in Mathematical Biology and Medicine, Vol 5) World Scientific, River Edge, NJ, pp 990–1008

Fitzurka MA, Tam DC (1996a) First order interspike interval difference phase plane analysis of neuronal spike train data. In: Bower JM (ed) Computational neuroscience. Academic Press, San Diego, pp 429–434

Fitzurka MA, Tam DC (1996b) Second order interspike interval difference phase plane analysis of neuronal spike train data. In: Bower JM (ed) Computational neuroscience. Academic Press, San Diego, pp 435–440

Fitzurka MA, Tam DC (1997) Hybrid analyses of neuronal spike train data for pre- and post-cross intervals in relation to interspike interval differences. In: Bower JM (ed) Computational neuroscience: trends in research. Academic Press, San Diego, pp 81–86

Gerstein GL, Kiang NY-S (1960) An approach to the quantitative analysis of electrophysiological data from single neurons. Biophys J 1:15–28

Gerstein GL, Perkel DH (1972) Mutual temporal relationships among neuronal spike trains. Biophys J 12:453–573

Gotton JM (1981) Time-series analysis: a comprehensive introduction for social scientists. Cambridge University Press, Cambridge, UK

Gray PR (1967) Conditional probability analyses of the spike activity of single neurons. Biophys J 7:759–777

Gross GW (1979) Simultaneous single unit recording in vitro with a photoetched, laser-deinsulated, gold multimicroelectrode surface. IEEE Trans Biomed Eng 26:273–279

Gross GW, Rieske E, Kreutzberg GW, Meyer A (1977) A new fixed-array multimicroelectrode system designed for long-term monitoring of extracellular single unit neuronal activity in vitro. Neurosci Lett 6:101–105

Kaluzny P, Tarnecki R (1993) Recurrence plots of neuronal spike trains. Biol Cybern 68:527–534

Longtin A, Hinzer K (1996) Encoding with bursting, subthreshold oscillations, and noise in mammalian cold receptors. Neural Comput 8:215–255

Maurer P, Wang H-D, Babloyantz A (1997) Time structure of chaotic attractors: a graphical view. Phys Rev E 56:1188–1196

Mayer-Kress G, Hubler A (1989) Time evolution of local complexity measures and aperiodic perturbations of nonlinear dynamical system. In: Agraham NB (ed) Quantitative measures of complex dynamical systems. Plenum, New York, pp 100–117

Moore GP, Perkel DH, Segundo JP (1966) Statistical analysis and functional interpretation of neuronal spike data. Annu Rev Physiol 28:493–522

Moore GP, Segundo JP, Perkel DH, Levitan H (1970) Statistical signs of synaptic interaction in neurons. Biophys J 10:876–900

Nomura T, Sato S, Doi S, Segundo JP, Stiber MD (1994) Global bifurcation structure of a Bonhoeffer-van der Pol oscillator driven by periodic pulse trains: comparison with data from a periodically inhibited biological pacemaker. Biol Cybern 72:55–67

Perkel DH, Gerstein GL, Moore GP (1967a) Neuronal spike trains and stochastic point processes. I. The single spike train. Biophys J 7:391–418

Perkel DH, Gerstein GL, Moore GP (1967b) Neuronal spike trains and stochastic point processes. II. Simultaneous spike trains. Biophys J 7:419–440

Perkel DH, Gerstein GL, Smith MS, Tatton WG (1975) Nerve-impulse patterns: a quantitative display technique for three neurons. Brain Res 100:271–296

Rodieck RW, Kiang NY-S, Gerstein GL (1962) Some quantitative methods for the study of spontaneous activity of single neurons. Biophys J 2:351–368

Rosenberg JR, Amjad AM, Breeze P, Brillinger DR, Halliday DM (1989) The Fourier approach to the identification of functional coupling between neuronal spike trains. Prog Biophys Mol Biol 53:1–31

Schulman JH, Thorson J (1964) On-line generation of joint-interval histogram. Rev Scientific Inst 35:1314–1315

Segundo JP, Moore GP, Stensaas L, Bullock TH (1963) Sensitivity of neurons in Aplysia to temporal patterns of arriving impulses. J Exp Biol 40:643–667

Segundo JP, Perkel DH, Moore GP (1966) Spike probability in neurones: influence of temporal structure in the train of synaptic events. Kybernetik 3:67–82

Segundo JP, Perkel DH, Wyman H, Hegstad H, Moore GP (1968) Input-output relations in computer-simulated nerve cells. Influence of the statistical properties, strength, number and interdependence of excitatory pre-synaptic terminals. Kybernetik 4:157–171

Segundo JP, Altshuler E, Stiber M, Garfinkel A (1991) Periodic inhibition of living pacemaker neurons. I. Locked, intermittent, messy, and hopping behaviors. Intl J Bifur Chaos 1:549–581

Segundo JP, Stiber M, Altshuler E, Vibert JF (1994) Transients in the inhibitory driving of neurons and their postsynaptic consequences. Neuroscience 62:459–480

Segundo JP, Vibert JF, Stiber M, Hanneton S (1995) Periodically modulated inhibition and its postsynaptic consequences. I. General features. Influence of modulation frequency. Neuroscience 68:657–692

Selz KA, Mandell AJ (1992) Critical coherence and characteristic times in brain stem neuronal discharge patterns. In: McKenna T, Davis J, Zornetzer S (eds) Single neuron computation. Academic Press, San Diego, pp 525–560

Shelhamer M (1997) On the correlation dimension of optokinetic nystagmus eye movements: computational parameters, filtering, nonstationarity, and surrogate data. Biol Cybern 76:237–250

Sherry CJ, Klemm WR (1982) Do neurons process information by relative intervals in spike trains? Neurosci Biobehav Rev 6:429–437

Sherry CJ, Klemm WR (1984) What is the meaningful measure of neuronal spike train activity? J Neurosci Methods 10:205–213

Smith CE (1992) A heuristic approach to stochastic models of single neurons. In: McKenna T, Davis J, Zornetzer S (eds) Single neuron computation. Academic Press, San Diego, pp 561–588

Sugihara G (1994) Nonlinear forecasting for the classification of natural time series. Philos Trans R Soc [Lond] A 348:477–465

Tam DC (1996) A time-scale invariant method for detection of changes and oscillations in neuronal firing intervals. In: Bower JM (ed) Computational neuroscience. Academic Press, San Diego, pp 465–470

Tam DC (1998) A cross-interval spike train analysis: the correlation between spike generation and temporal integration of doublets. Biol Cybern 78:95–106

Tam DC, Ebner TJ, Knox CK (1988) Cross-interval histogram and cross-interspike interval histogram correlation analysis of simultaneously recorded multiple spike train data. J Neurosci Methods 23:23–33

Terasawa M, Tsukada M, Hauske G (1989) Temporal pattern discrimination within the receptive field of cat retinal ganglion cells. Biol Cybern 60:239–246

Tsukada M, Ishii N, Sato R (1975) Temporal pattern discrimination of impulse sequences in the computer-simulated nerve cells. Biol Cybern 17:19–28

Tsukada M, Terasawa M, Hauske G (1982) Temporal pattern sensitive and nonsensitive responses in the cat's retinal ganglion cells. Biol Cybern 44:197–203

Tsukada M, Terasawa M, Hauske G (1983) Temporal pattern discrimination in cat's retinal cells and Markov system models. IEEE Trans SMC-13:953–964

Tuckwell HC (1988) Introduction to theoretical neurobiology, Vol 2. Nonlinear and stochastic theories. Cambridge University Press, Cambridge, UK

Yang GL, Chen TC (1978) On statistical methods in neuronal spike train analysis. Math Biosci 38:1–34